IOP Publishing Journal of Physics: Condensed Matter
J. Phys.: Condens. Matter **27** (2015) 206002 (5pp) doi:10.1088/0953-8984/27/20/206002

The magnetic structure of $EuCu_2Sb_2$

D H Ryan[1], J M Cadogan[2], V K Anand[3], D C Johnston[3] and R Flacau[4]

[1] Centre for the Physics of Materials and Physics Department, McGill University, Montréal, QC, H3A 2T8, Canada
[2] School of Physical, Environmental and Mathematical Sciences, UNSW Canberra at the Australian Defence Force Academy, Canberra, BC 2610, ACT, Australia
[3] Ames Laboratory and Department of Physics and Astronomy, Iowa State University, Ames, Iowa 50011, USA
[4] Canadian Neutron Beam Centre, Chalk River Laboratories, Chalk River, ON, K0J 1J0, Canada

E-mail: dhryan@physics.mcgill.ca

Received 23 February 2015, revised 25 March 2015
Accepted for publication 30 March 2015
Published 6 May 2015

Abstract

Antiferromagnetic ordering of $EuCu_2Sb_2$ which forms in the tetragonal $CaBe_2Ge_2$-type structure (space group P4/nmm #129) has been studied using neutron powder diffraction and ^{151}Eu Mössbauer spectroscopy. The room temperature ^{151}Eu isomer shift of $-12.8(1)$ mm s^{-1} shows the Eu to be divalent, while the ^{151}Eu hyperfine magnetic field (B_{hf}) reaches 28.7(2) T at 2.1 K, indicating a full Eu^{2+} magnetic moment. B_{hf}(T) follows a smooth $S = \frac{7}{2}$ Brillouin function and yields an ordering temperature of 5.1(1) K. Refinement of the neutron diffraction data reveals a collinear A-type antiferromagnetic arrangement with the Eu moments perpendicular to the tetragonal c-axis. The refined Eu magnetic moment at 0.4 K is 7.08(15) μ_B which is the full free-ion moment expected for the Eu^{2+} ion with $S = \frac{7}{2}$ and a spectroscopic splitting factor of $g = 2$.

Keywords: Mössbauer spectroscopy, neutron diffraction, magnetic structure, rare earth intermetallics, pnictides

(Some figures may appear in colour only in the online journal)

1. Introduction

The rare-earth pnictides are enjoying considerable interest following the discovery of superconductivity in the FeAs-based compounds [1]. It is clear that there is a complex interplay between magnetism, superconductivity and crystallography in both the pnictide and chalcogenide rare-earth compounds and compounds such as $EuFe_2As_2$, for example, present a good opportunity to study this interplay due to the presence of a magnetic moment on the rare-earth atom (in this case Eu).

In this paper we study the magnetic analogue of these superconductors, $EuCu_2Sb_2$, which crystallises in the $CaBe_2Ge_2$-type primitive tetragonal structure with the space group $P4/nmm$ (#129). There is one Eu site ($2c$), two Cu sites ($2a$ and $2c$) and two Sb sites ($2b$ and $2c$) [2, 3]. Magnetic ordering occurs at a Néel temperature of 5.1 K [2]. Based on single-crystal magnetisation measurements, the antiferromagnetic structure was suggested to be either a collinear A-type structure or a coplanar helical structure with the axis of the helix along the crystallographic c-axis. In both possible structures the ordered moments are predicted to lie in the ab-plane.

Here, we determine directly the magnetic structure of $EuCu_2Sb_2$ using a combination of neutron powder diffraction and ^{151}Eu Mössbauer spectroscopy. Our results confirm the suggestion of A-type planar antiferromagnetism.

2. Experimental methods

The polycrystalline sample of $EuCu_2Sb_2$ was synthesized by the solid state reaction method starting with high purity elements (Eu: Ames Lab, Cu: 99.999% Alfa Aesar, Sb: 99.999 99% Alfa Aesar). The Eu was cut into small pieces and mixed with powders of Cu and Sb in the stoichiometric ratio 1:2:2, pelletized and sealed in an evacuated quartz tube which was sintered at 900 °C for 30 h with two subsequent grinding, pelletizing, sealing and sintering processes at 900 °C for 60 h each.

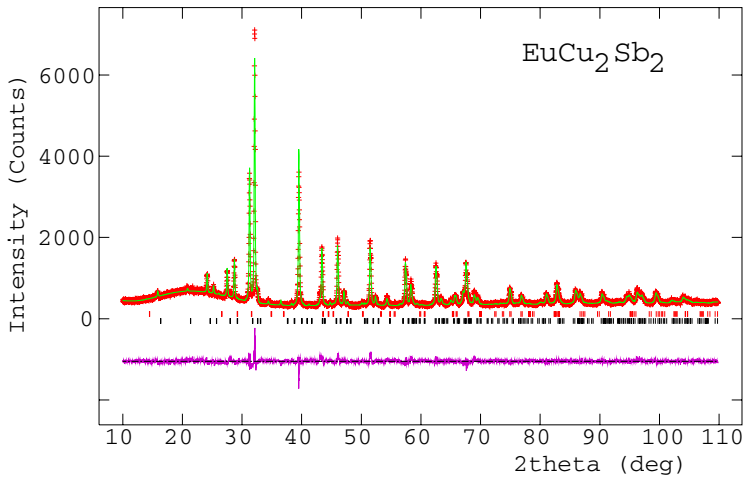

Figure 1. X-ray powder diffraction pattern (CuK_α) of $EuCu_2Sb_2$, collected at 298 K. The two rows of Bragg markers represent the primary $EuCu_2Sb_2$ phase (bottom row, black) and a 3.5(2) wt.% Cu_2Sb impurity phase (top row, red).

X-ray powder diffraction (Cu-K_α) was used to verify the structure and phase composition of the sample. The diffraction pattern was fitted using the GSAS/EXPGUI package [4, 5].

Neutron powder diffraction experiments were carried out on the C2 800-wire powder diffractometer (DUALSPEC) at the NRU reactor, Chalk River Laboratories, Ontario, Canada, using a neutron wavelength (λ) of 1.3286(2) Å. Some patterns were also collected with $\lambda = 2.3789(2)$ Å to confirm that no low-2θ peaks had been missed with the shorter λ. Diffraction patterns were obtained over the temperature range 0.4–10 K using a closed-cycle ^{3}He 'Heliox' cryostat manufactured by Oxford Instruments. The neutron diffraction patterns were analysed using the Rietveld method and the *FullProf/WinPLOTR* program [6, 7]. Natural europium is a strong neutron absorber and its scattering length is dependent on the neutron energy, as tabulated by Lynn and Seeger [8], from which we derived the scattering length coefficient appropriate to our neutron wavelength ($\lambda = 1.33$ Å, $E = 46.2$ meV), namely $6.9 - 0.9i$ fm. The sample mounting arrangement for this strongly-absorbing sample employs a large-area, flat-plate geometry as outlined in a previous paper [9] and used by us in neutron diffraction studies of other Eu 1:2:2 compounds [10, 11]. The determination of the symmetry-allowed magnetic structures by Representational Analysis used the BASIREPS program [6, 7].

The ^{151}Eu Mössbauer spectroscopy measurements were carried out using a 4 GBq $^{151}SmF_3$ source, driven in sinusoidal-mode. The drive motion was calibrated using a standard ^{57}CoRh/α-Fe foil. The 21.6 keV gamma rays were recorded using a thin NaI scintillation detector. The sample was cooled in a helium flow cryostat. Temperature stability, as read by a calibrated cernox thermometer, was better than 0.01 K during each measurement. The spectra were fitted using a conventional non-linear least-squares minimisation routine to a sum of Lorentzian lines with positions calculated from the nuclear Hamiltonian [12]. No quadrupole term was used to fit the spectra.

Estimates of the magnetic ordering temperature were derived from fits to the temperature dependence of the ^{151}Eu hyperfine field and the intensities of several strong magnetic reflections in the neutron diffraction patterns. We used a conventional molecular field approximation and assumed that the local moments responded according to a $S = \frac{7}{2}$ Brillouin function. For brevity, this is referred to as a fit to a '$S = \frac{7}{2}$ Brillouin function' in the figure captions.

3. Results and discussion

3.1. Structural characterisation

Analysis of the x-ray diffraction pattern shown in figure 1 confirmed the expected tetragonal $CaBe_2Ge_2$-type structure (space group P4/nmm #129), and gave lattice parameters and atomic positions that were fully consistent with those of Dünner *et al* [3] (see table 1). We found no evidence for the smaller cell reported for crushed single crystals, nor did we see any indication of vacancies on the Cu(2c) site [2]. A free fit to the occupancies of the two copper sites gave 1.029(12) and 0.995(13) for the Cu(2a) and Cu(2c) sites respectively. These are not significantly different from unity and full occupation was assumed in the final refinement. A small (3.5(2) wt.%) Cu_2Sb impurity phase was detected in the analysis of the x-ray diffraction data, but as this is non-magnetic, it cannot affect the analysis of the magnetic structure. It was also possible to include about 1 wt.% of Eu_2O_3 but this had no impact on the quality of the fit and did not appear to be contributing to any missed peak in the data, so it was not included in the final analysis presented in figure 1 and table 1.

3.2. ^{151}Eu Mössbauer spectroscopy

Figure 2 shows our ^{151}Eu Mössbauer spectrum of $EuCu_2Sb_2$ obtained at 2.09 K (below the Néel temperature of 5.1 K). It is clear from the isomer shift ($-12.8(1)$ mm s^{-1} at 298 K) that the Eu is in a divalent $4f^7$ electronic state with orbital angular momentum $L = 0$ and spin $S = \frac{7}{2}$ [13, 14]. The ^{151}Eu hyperfine magnetic field at 2.09 K is 28.7(2) T and in figure 3 we show the temperature dependence of this hyperfine field which yields a magnetic ordering temperature of 5.09(2) K, in

Table 1. Crystallographic data for $EuCu_2Sb_2$ obtained by refinement of the 298 K x-ray powder diffraction pattern.

Atom	Site	x	y	z
Eu	2c	1/4	1/4	0.2388(3)
Cu	2a	3/4	1/4	0
Cu	2c	1/4	1/4	0.6389(6)
Sb	2b	3/4	1/4	1/2
Sb	2c	1/4	1/4	0.8697(3)

$a = 4.50445(11)$ Å $c = 10.8287(4)$ Å
$V_{cell} = 219.72(1)$ Å^3
$\chi^2 = 2.15$
$R_{wp} = 6.52\%$
R(F) = 8.57%

Note: The space group is tetragonal $P4/nmm$ (#129).

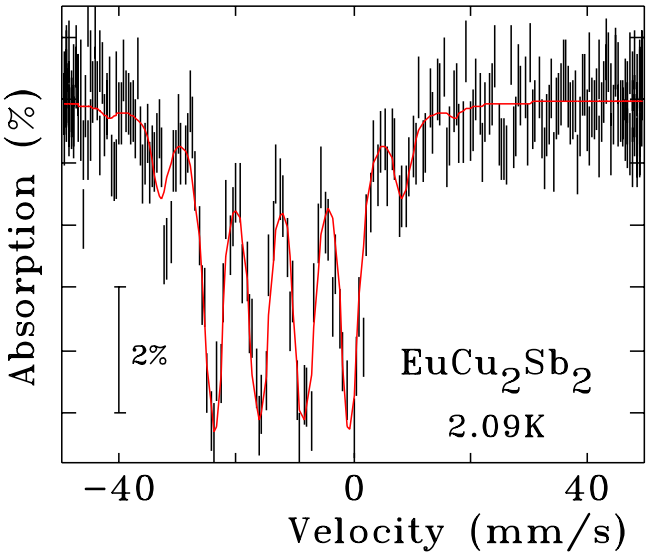

Figure 2. ^{151}Eu Mössbauer spectrum of $EuCu_2Sb_2$ obtained at 2.09 K. The solid (red) line shows the full-Hamiltonian fit to this spectrum.

excellent agreement with the previous susceptibility and heat-capacity results [2].

3.3. Neutron powder diffraction

The neutron powder diffraction patterns of $EuCu_2Sb_2$ obtained at 10 K (above the Néel temperature) and 0.4 K (below the Néel temperature) are shown in figure 4. The figure also shows the difference between these two patterns, illustrating the significant magnetic diffraction from the Eu sublattice. The magnetic contribution to the pattern obtained at 0.4 K is quite striking, particularly the very large, almost purely magnetic peak that occurs at $2\theta = 7^\circ$ ($d = 10.8$ Å). This peak indexes as (0 0 1), showing that the Eu magnetic moments do not lie along the tetragonal c-axis.

Figure 5 shows the temperature dependences of the principal magnetic contributions to the neutron diffraction patterns, namely the (0 0 1) peak at $2\theta = 7.05^\circ$, the (0 1 0) at $2\theta = 17.05^\circ$ and the (0 1 2) at $2\theta = 22.2^\circ$ (with $\lambda = 1.3286$ Å). These curves yield an average Néel temperature of 5.10(3) K, in perfect agreement with that obtained from the

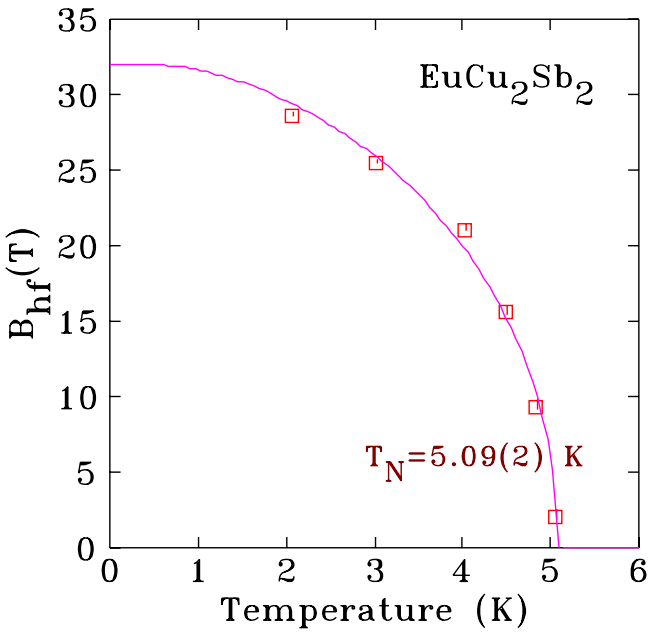

Figure 3. Temperature dependence of the ^{151}Eu hyperfine magnetic field in $EuCu_2Sb_2$. The solid (magenta) line is a fit to an $S = \frac{7}{2}$ Brillouin function.

temperature dependence of the ^{151}Eu hyperfine magnetic field, and with the value in [2].

The full refinement of the neutron diffraction pattern measured at 10 K is shown in figure 6. At this temperature, $EuCu_2Sb_2$ is paramagnetic so this pattern comprises only nuclear scattering. In addition to the primary $EuCu_2Sb_2$ phase, we also detected small amounts of Cu_2Sb (2.5(3) wt.%) and Eu_2O_3 (0.9(2) wt.%). These were included in the fits and the Bragg markers associated with these impurities are shown on the figures. As with the x-ray diffraction data, we found no evidence for copper vacancies. A free fit to the occupancies of the two copper sites gave 1.015(19) and 0.989(20) for the Cu(2a) and Cu(2c) sites, respectively. These are not significantly different from unity and full occupation was therefore assumed in refining the neutron diffraction data.

In figure 7 we show the full refinement of the neutron diffraction pattern of $EuCu_2Sb_2$ obtained at 0.4 K. This pattern shows several strong peaks representing the magnetic scattering from the Eu sublattice. As noted earlier, the dominant peak at $2\theta = 7^\circ$ indexes as (0 0 1) and is overwhelmingly magnetic in origin (99.3% of the total intensity is from the magnetic scattering). Thus, we may conclude that the ordered moments of the Eu sublattice in $EuCu_2Sb_2$ are not oriented parallel to the tetragonal c-axis.

All magnetic contributions were found to correspond to a propagation vector $\mathbf{k} = [0\,0\,0]$. To verify that there were no lower-angle peaks that would indicate a longer period or incommensurate magnetic structure, we also obtained a diffraction pattern at 0.4 K using the longer neutron wavelength of 2.3789(2) Å (not shown here). To determine the allowed magnetic orientations of the Eu(2c) moments with the $\mathbf{k} = [0\ 0\ 0]$ propagation vector we carried out Representational Analysis using the BASIREPS program [6, 7]. The magnetic representation for the Eu(2c) site

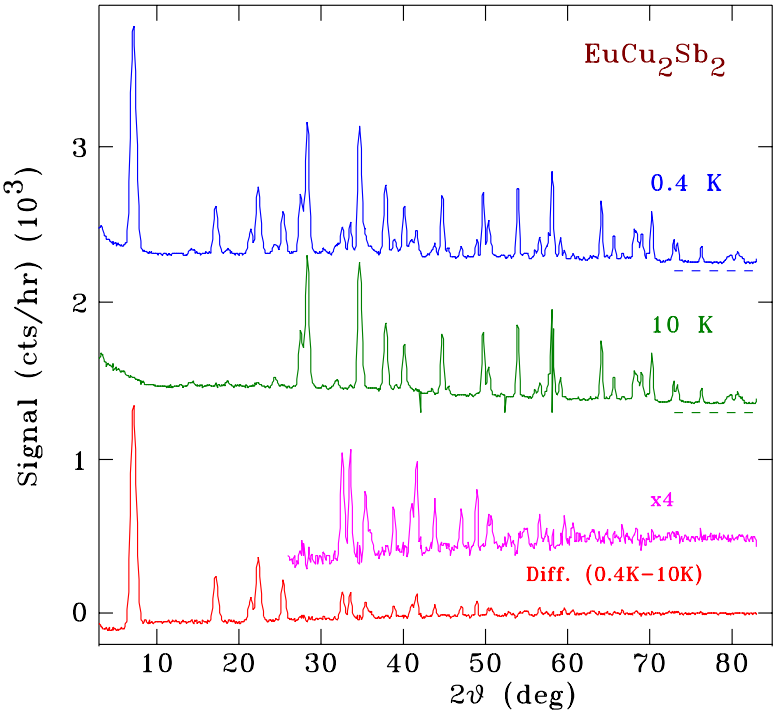

Figure 4. Neutron powder diffraction patterns of $EuCu_2Sb_2$ obtained at 10 K (middle-green) and 0.4 K (top-blue). We also show the difference pattern (bottom-red) which represents the magnetic scattering from the Eu sublattice at 0.4 K. We also show the difference pattern at higher angles scaled up by a factor of 4 (purple). These patterns have been offset vertically for clarity and the dashed horizontal lines give the experimental baselines for the 0.4 K and 10 K patterns.

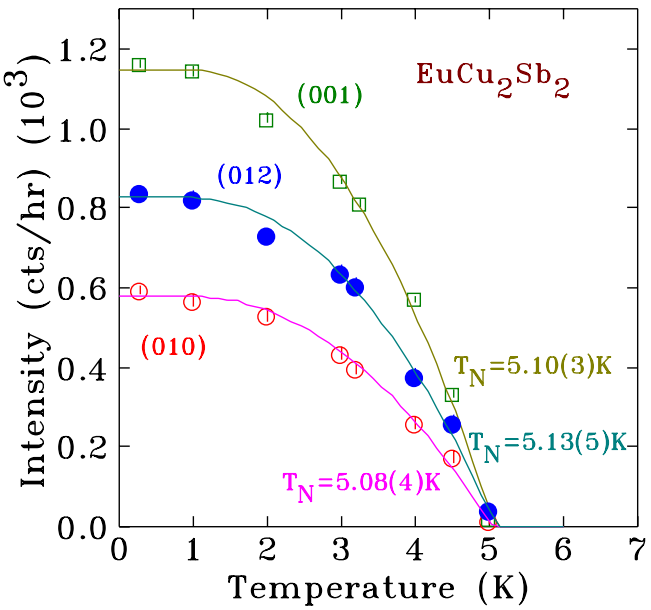

Figure 5. Temperature dependence of the peak intensities of three main magnetic contributions to the neutron powder diffraction patterns of $EuCu_2Sb_2$. The intensities of the (0 1 0) and (0 1 2) peaks have been increased by a factor of 3. The solid lines are fits to $S = \frac{7}{2}$ squared Brillouin functions.

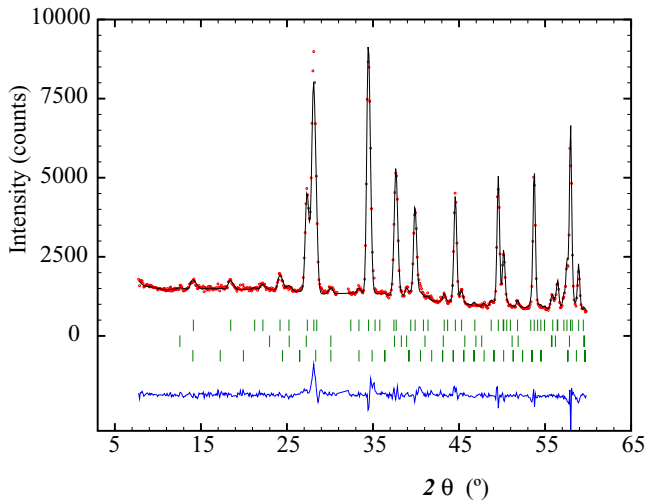

Figure 6. Refinement of the neutron powder diffraction pattern of $EuCu_2Sb_2$ obtained at 10 K with a neutron wavelength of 1.3286(3) Å. The rows of Bragg markers show the positions of the diffraction peaks from the primary $EuCu_2Sb_2$ phase (top), Cu_2Sb middle and Eu_2O_3 (bottom). The blanked out feature around $2\theta = 32^\circ$ is an experimental artefact.

comprises four representations, two 1-dimensional and two 2-dimensional:

$$\Gamma^{2c}_{\text{Mag}} = 1\Gamma^{(1)}_2 + 1\Gamma^{(1)}_7 + 1\Gamma^{(2)}_9 + 1\Gamma^{(2)}_{10} \qquad (1)$$

The basis vectors of these irreducible representations are given in table 2.

Representational Analysis shows that the allowed ordering mode of the Eu(2c) moments is either *ab*-planar or *c*-axial. The best refinement to the 0.4 K diffraction pattern was for the Eu(2c) sublattice ordered with a propagation vector [0 0 0] with the Eu(2c) magnetic moments in the *ab*-plane. This corresponds to the $\Gamma^{(2)}_9$ representation. While it is possible to distinguish axial ordering from planar

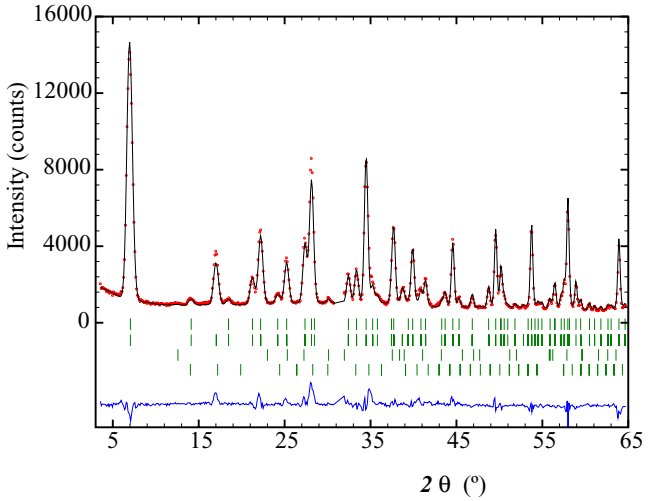

Figure 7. Refinement of the neutron powder diffraction pattern of $EuCu_2Sb_2$ obtained at 0.4 K with a neutron wavelength of 1.3286(2) Å. The rows of Bragg markers show the positions of the diffraction peaks from (working from top to bottom): nuclear scattering from the primary $EuCu_2Sb_2$ phase, magnetic scattering from the primary $EuCu_2Sb_2$ phase, Cu_2Sb and Eu_2O_3. The blanked out feature around $2\theta = 32^\circ$ is an experimental artefact.

Table 2. Representational Analysis for the Eu(2c) site in $EuCu_2Sb_2$ with a propagation vector [0 0 0].

Representation	Ordering
$\Gamma_2^{(1)}$	$[0\ 0\ z] + [0\ 0\ \overline{z}]$
$\Gamma_7^{(1)}$	$[0\ 0\ z] + [0\ 0\ z]$
$\Gamma_9^{(2)}$	$[x\ \overline{y}\ 0] + [\overline{x}\ y\ 0]$
$\Gamma_{10}^{(2)}$	$[x\ y\ 0] + [x\ y\ 0]$

Note: The atomic positions of the Eu moments are (1/4, 1/4, z) and (3/4, 3/4, $\overline{z}$).

ordering, tetragonal symmetry precludes the determination of the orientation of the ordered moments within the *ab*-plane [15]. Our fitted magnetic structure consists of ferromagnetic sheets of moments in the *ab*-plane that are aligned antiferromagnetically along the *c*-axis: the A-type antiferromagnet predicted on the basis of bulk magnetic measurements [2].

The refined Eu magnetic moment at 0.4 K is 7.08(15) μ_B, the free-ion moment expected for an $S = \frac{7}{2}$ Eu^{2+} configuration. The refined lattice parameters at 0.4 K are $a = 4.481(1)$ Å and $c = 10.805(5)$ Å. The conventional R-factors for this refinement are R(Bragg) = 15.0%, R(F) = 8.5% and R(mag) = 6.3%. The structural and magnetic refinement of the 0.4 K diffraction pattern is shown in figure 7.

4. Conclusions

We have used neutron powder diffraction and ^{151}Eu Mössbauer spectroscopy to determine the magnetic structure of $EuCu_2Sb_2$. We find that this pnictide compound adopts an A-type antiferromagnet structure below 5.1(1) K. The Eu^{2+} magnetic moments are aligned in the tetragonal basal plane with a propagation vector $k = [0\,0\,0]$, and at 0.4 K have the free-ion moment of 7.08(15) μ_B.

Acknowledgments

We thank A I Goldman and A Kreyssig for helpful discussions. Financial support for this work was provided by the Natural Sciences and Engineering Research Council of Canada, the Fonds Québécois de la Recherche sur la Nature et les Technologies and The University of New South Wales. DHR acknowledges the award of a Rector-funded Visiting Fellowship by UNSW Canberra. Work at Ames Laboratory is supported by the US Department of Energy, Office of Basic Energy Sciences, Division of Materials Sciences and Engineering. Ames Laboratory is operated for the US Department of Energy by Iowa State University under Contract No. DE-AC02-07CH11358.

References

[1] Johnston D C 2010 *Adv. Phys.* **59** 803
[2] Anand V K and Johnston D C 2015 Antiferromagnetism in $EuCu_2As_2$ and $EuCu_2Sb_2$ single crystals *Phys. Rev. B* arXiv:1503.06074 submitted
[3] Dünner J, Mewis A, Roepke M and Michels G 1995 *Z. Anorg. Allg. Chem.* **621** 1523
[4] Larson A C and Von Dreele R B 2000 General structure analysis system (GSAS) Los Alamos National Laboratory *Report* LAUR 86-748
[5] Toby B H 2001 *J. Appl. Cryst.* **34** 210
[6] Rodríguez-Carvajal J 1993 *Physica* B **192** 55
[7] Roisnel T and Rodríguez-Carvajal J 2001 *Mater. Sci. Forum* **378–81** 118
[8] Lynn J E and Seeger P A 1990 *At. Data Nucl. Data Tables* **44** 191
[9] Ryan D H and Cranswick L M D 2008 *J. Appl. Cryst.* **41** 198
[10] Ryan D H, Cadogan J M, Xu S and Cao G 2011 *Phys. Rev.* B **83** 132403
[11] Rowan-Weetaluktuk W N, Ryan D H, Lemoine P and Cadogan J M 2014 *J. Appl. Phys.* **115** 17E101
[12] Voyer C J and Ryan D H 2006 *Hyperfine Interact.* **170** 91
[13] Bauminger E R, Kalvius G M and Nowik I 1978 *Mössbauer Isomer Shifts* ed G K Shenoy and F E Wagner (New York: North Holland) pp 661–756
[14] Grandjean F and Long G J 1989 *Mössbauer Spectroscopy Applied to Inorganic Chemistry* vol 3 ed G J Long and F Grandjean (New York: Plenum) pp 513–90
[15] Shirane G 1959 *Acta Cryst.* **12** 282